PAPER

Band gap narrowing in nitrogen-doped La$_2$Ti$_2$O$_7$ predicted by density-functional theory calculations†

Junying Zhang,*[a] Wenqiang Dang,[a] Zhimin Ao,[b] Scott K. Cushing[c] and Nianqiang Wu*[c]

In order to reveal the origin of enhanced photocatalytic activity of N-doped La$_2$Ti$_2$O$_7$ in both the visible light and ultraviolet light regions, its electronic structure has been studied using spin-polarized conventional density functional theory (DFT) and the Heyd–Scuseria–Ernzerhof (HSE06) hybrid approach. The results show that the deep localized states are formed in the forbidden band when nitrogen solely substitutes for oxygen. Introducing the interstitial Ti atom into the N-doped La$_2$Ti$_2$O$_7$ photocatalyst still causes the formation of a localized energy state. Two nitrogen substitutions co-exist stably with one oxygen vacancy, creating a continuum energy band just above the valence band maximum. The formation of a continuum band instead of mid-gap states can extend the light absorption to the visible light region without increasing the charge recombination, explaining the enhanced visible light performance without deteriorating the ultraviolet light photocatalytic activity.

1. Introduction

Since the discovery of photocatalysis by Fujishima and Honda,[1] semiconductor-based materials have found a wide range of applications in removing organic pollutants from water and air, splitting water into hydrogen and oxygen, as well as reducing CO$_2$.[2–4] Of the numerous photocatalysts, layer-structured semiconductors have received extensive attention because the reduction and oxidation reactions, *e.g.* H$_2$ and O$_2$ evolution sites, are separated out.[5–7] Perovskite-type photocatalysts consist of the network of corner-sharing octahedra that is beneficial to the mobility of charge carriers, leading to high photocatalytic activity.[8–10] Perovskite-type La$_2$Ti$_2$O$_7$ with a layered structure possesses the merits of both perovskite and layered structures, which exhibits high photocatalytic activity toward organic decomposition, water splitting and CO$_2$ reduction. For example, layered perovskite La$_2$Ti$_2$O$_7$(110) loaded with nickel showed a quantum yield as high as 12%

in water splitting under ultraviolet (UV) irradiation, which exhibited much better photocatalytic activity than Pt-loaded TiO$_2$.[5] In the absence of a co-catalyst, La$_2$Ti$_2$O$_7$ nanosheets demonstrated similar activity to Degussa P25 in photocatalytic hydrogen evolution from the water–ethanol solution.[11] It has also been reported that 98% of Cr(VI) ions in water was removed by La$_2$Ti$_2$O$_7$ after 3 hours of UV irradiation.[12]

La$_2$Ti$_2$O$_7$ has a wide band gap (3.0–4.0 eV), which depends on the synthesis method and the resulting morphology.[5,11,13–19] Hence it shows photocatalytic activity only under UV light irradiation. Rh-doped La$_2$Ti$_2$O$_7$ was active for H$_2$ evolution from an aqueous methanol solution under visible light irradiation owing to the photo-excitation of localized energy levels resulting from the Rh^{3+}doping.[14] Similarly, Cr and/or Fe doping in La$_2$Ti$_2$O$_7$ induced intensive light absorption in the visible light region and photocatalytic hydrogen production from the water–methanol solution due to the formation of a partially filled 3d band in the band gap.[17,20] The recent experimental results demonstrated that the nitrogen-doped La$_2$Ti$_2$O$_7$ nanosheets not only showed significant visible light photocatalytic activity but also exhibited enhanced ultraviolet light photocatalytic activity.[13,21] Nitrogen doping in La$_2$Ti$_2$O$_7$ narrowed the band gap rather than creating the localized mid-gap states, which was different from N-doped anatase TiO$_2$. These results could not be explained by the first-principles calculations, which showed that nitrogen substituting for oxygen caused the formation of the localized energy state in the band gap of La$_2$Ti$_2$O$_7$.[22,23] Since the energy band gap is a critical factor

[a] *Department of Physics, Beihang University, Beijing 100191, China.*
  E-mail: zjy@buaa.edu.cn; Fax: +86-10-82317931; Tel: +86-10-82315351
[b] *Center for Clean Energy Technology, School of Chemistry and Forensic Science,*
  University of Technology Sydney, P.O. Box 123, Broadway, Sydney, NSW 2007,
  Australia
[c] *Department of Mechanical and Aerospace Engineering, West Virginia University,*
  Morgantown, WV 26506-6106, USA. E-mail: nick.wu@mail.wvu.edu;
  Tel: +1-304-293-3326
† Electronic supplementary information (ESI) available. See DOI: 10.1039/c5cp00157a

8994 | *Phys. Chem. Chem. Phys.*, 2015, **17**, 8994–9000

This journal is © the Owner Societies 2015

governing the photocatalytic activity, and doping is the most common method for altering the energy band gap,[2] it is essential to understand the effect of doping on the electronic band structure of a semiconductor.

Herein, we investigate the influence of N-doping on the crystal and the electronic structures of $La_2Ti_2O_7$ using first-principles calculations. We assume that nitrogen substitutes for oxygen when it is doped in $La_2Ti_2O_7$ based on the experimental evidence.[13] We check whether deep trap states will be formed in the forbidden band when nitrogen solely replaces oxygen. We also examine whether a localized energy state will still exist when the nitrogen substitutions co-exist with interstitial Ti atoms. Furthermore, we explore how the oxygen vacancies are used to stabilize the dopants, leading to an enhancement of visible light absorption without reducing the lifetime of the charge carrier. In particular, we investigate what is the case if one oxygen vacancy (V_O) stably exists with two nitrogen substitutions (N_S).

2. Calculation methods

The calculations have been performed using the Vienna *ab initio* simulation program (VASP).[24] Adopting the Perdew–Burke–Ernzerhof (PBE) prescription, the generalized gradient approximation (GGA) was used to represent the electronic exchange–correlation energy during the geometry relaxation.[25] The hybrid-functional Heyd–Scuseria–Ernzerhof (HSE06) method[26] was also employed to calculate the electronic structure. The projector-augmented-wave (PAW) potentials were used to describe the electron–ion interactions.[27] The valence configurations including valence and semicore electrons were $2s^2 2p^4$ for oxygen, $2s^2 2p^3$ for nitrogen, $3p^6 3d^3 4s^1$ for titanium and $5s^2 5p^6 5d^1 6s^2$ for lanthanum. The cut-off energy was 450 eV and the Monkhorst–Pack k-point mesh was $6 \times 8 \times 4$ for a 44-atom supercell. Structural relaxations were performed until the self-consistent total energy difference reached 10^{-5} eV and the residual forces on atoms fell below 0.02 eV Å^{-1}.

3. Results and discussion

The monoclinic $La_2Ti_2O_7$ has a layered perovskite structure with $P21$ space group. The calculated lattice parameters using GGA are, respectively, $a = 7.795$ Å, $b = 5.604$ Å and $c = 13.264$ Å (Fig. 1(a)), agreeing well with the experimental values of $a = 7.812$ Å, $b = 5.5440$ Å, and $c = 13.010$ Å.[28] For the supercell containing 44 atoms, there were 14 lattice sites of the oxygen atom for nitrogen to enter, giving rise to a doping concentration of 3.6 at% similar to the experimental value.[13] We calculated the total energies for all the 14 configurations, and the relaxed geometry with the minimum total energy is shown in Fig. 1(b). It can be seen that doping N into $La_2Ti_2O_7$ had little influence on the crystal structure.

Fig. 2 shows the density of states (DOS) of pristine $La_2Ti_2O_7$ resulting from the calculations of the conventional DFT and the HSE06 hybrid function. It can be seen that the components of

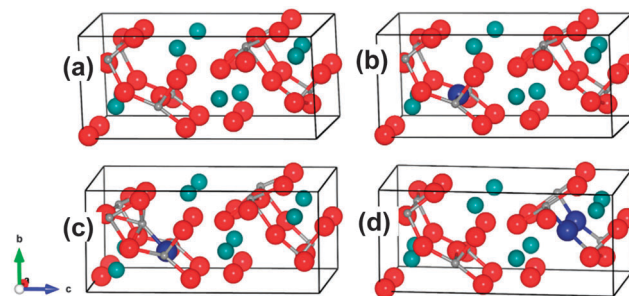Fig. 1 Supercells showing the optimized crystal structures of pristine $La_2Ti_2O_7$ (a), N-doped $La_2Ti_2O_7$ (b), $La_2Ti_2O_7$ with the $N_S + Ti_i$ complex (c) and $La_2Ti_2O_7$ with complex defects ($2N_S + V_O$) (d). The grey, red, light-blue and blue spheres denote the Ti, O, La, and N atoms, respectively.
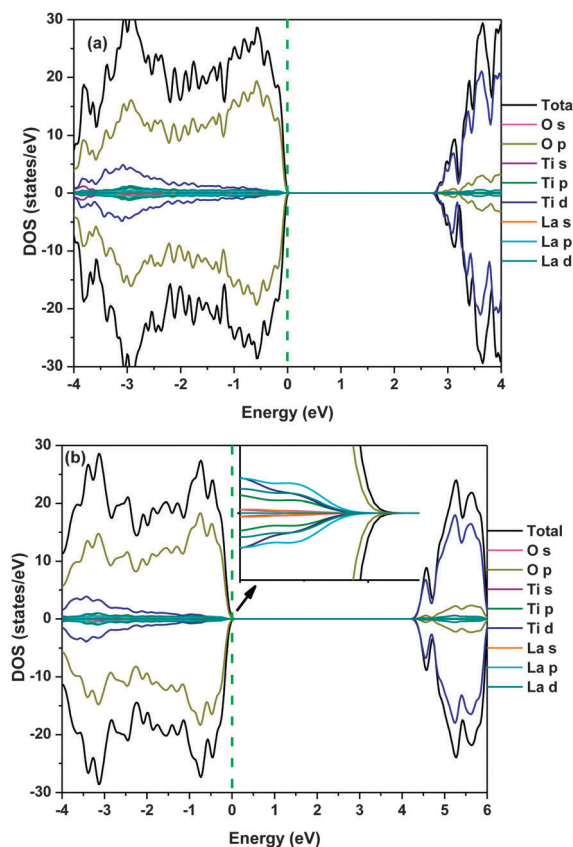

Fig. 2 DOS of pristine $La_2Ti_2O_7$ calculated using the conventional DFT (a) and the HSE06 method (b). The dash line annotates the Fermi level.

the DOS curves obtained with the two methods were very similar. The valence band maximum was composed of O 2p in majority and Ti 3p, Ti 3d and La 5p, La 5d in minority. The conduction band minimum was mainly constructed by Ti 3d with minor O 2p and a few La 5d states. Since all the elements contribute to the valence band maximum (VBM) and the conduction band minimum (CBM), the subtle stoichiometric change, *e.g.* by doping other elements, forming the vacancies or interstitial atoms, will definitely affect the electronic structure of the system.

The indirect band gap of pristine $La_2Ti_2O_7$ calculated using the conventional DFT was 2.9 eV (Fig. 3(a)), underestimating

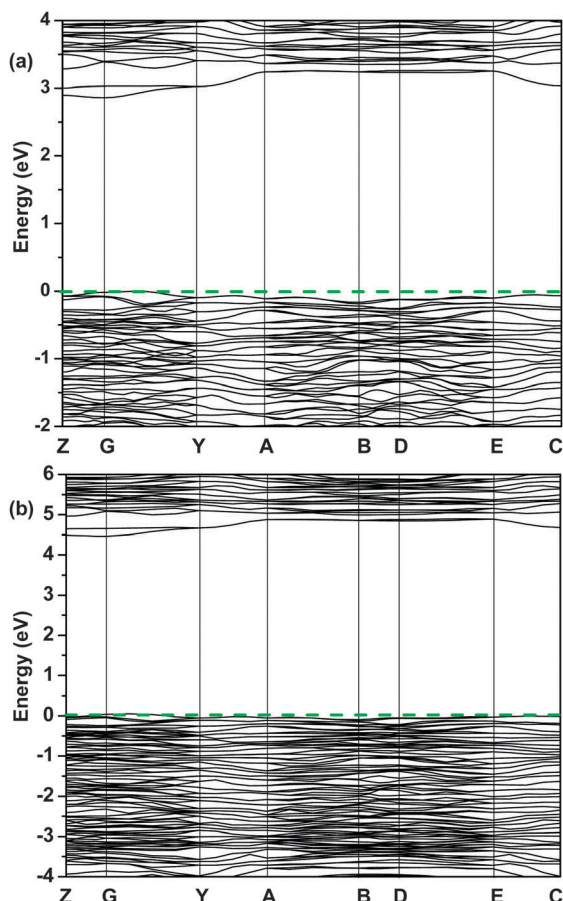**Fig. 3** Band structure of pristine $La_2Ti_2O_7$ calculated using the conventional DFT (a) and the HSE06 method (b). The dash line annotates the Fermi level.

the experimental value due to the well-known limitations in the conventional DFT.[29,30] When the HSE06 hybrid method was used, the calculated band gap was 4.4 eV (Fig. 3(b)), which was slightly larger than the typical experimental value obtained with the solid-state reaction (3.8 eV)[14] and the molten salt synthesis method (3.9 eV).[15]

Fig. 4 and Fig. S1 (ESI†) reveal the DOS and the band structure of N-doped $La_2Ti_2O_7$. The zero energy point was set to the Fermi level of pristine $La_2Ti_2O_7$. The systems with defects were corrected by aligning the average electrostatic potential (V_{av}) of La, Ti and O atoms located far from the defects and the V_{av} of same elements in the pristine $La_2Ti_2O_7$.[31] When N substituted for O to form the N_S defect, the localized deep energy states appeared in the middle of the forbidden band, which came from the mixture of N 2p, O 2p, Ti 3d and La 5d orbitals. Furthermore, Fig. 4(c) shows that the Ti d orbitals were hybridized with the N p orbitals at the VBM. As a result, mixing of N, O, Ti and La orbitals caused the add-on of shallow states above the VBM. Band gap narrowing of 0.30 eV and 0.41 eV occurred in comparison with the pristine material, respectively, for the value calculated using the conventional DFT and HSE06 methods. The N_S defect shifted the direct transition at the G point to a similar energy as the indirect transition near the B
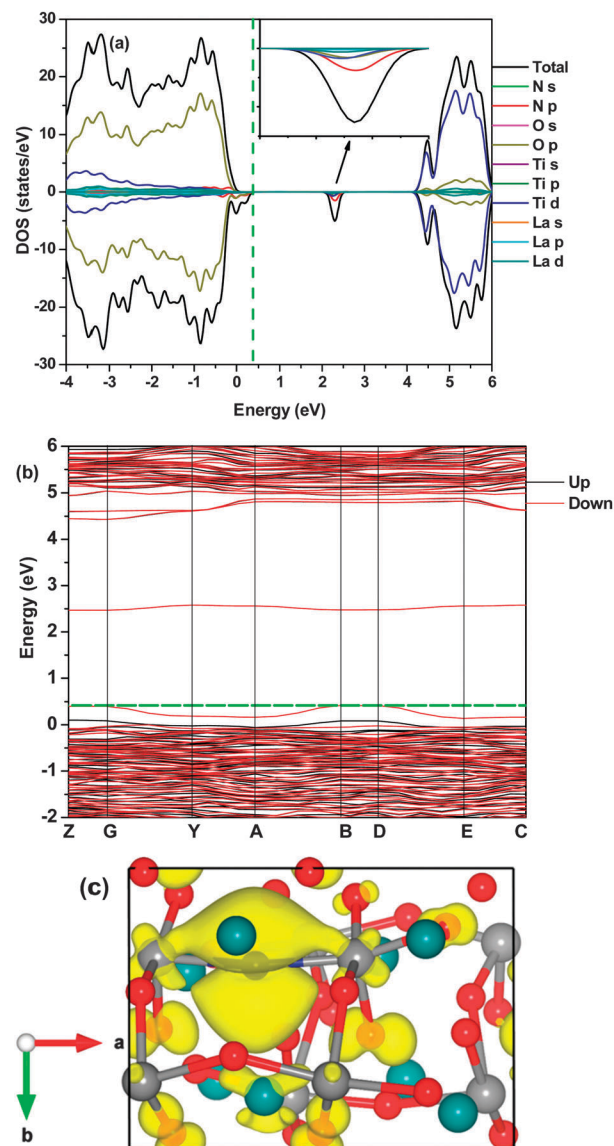

Fig. 4 DOS (a), band structure (b) and partial electron density of the VBM at a 0.01 eV $Å^{-3}$ isosurface level (c) of $La_2Ti_2O_7$ with the N_S defect calculated using the HSE06 method. The dash line annotates the Fermi level.

and D points, comparing Fig. 3 with 4, allowing a larger increase in absorption near the band edge. Since N requires one more electron than an O atom from the $La_2Ti_2O_7$ lattice, the unequal up and down-spin electrons result in the asymmetric DOS curve. These results agreed with the previous results calculated using the HSE06 method.[22,23] In TiO_2, first-principles calculations also showed that N_S produced the deep localized states in the band gap,[32–34] similar to the results of this work. The deep localized energy band was the un-occupied state. It can induce the limited visible light photocatalytic activity but it generally has an adverse effect on the UV light photocatalytic activity since the mid-gap states can act as the charge traps.[35]

Recently, the DFT plus the onsite Coulomb interaction (U) calculations show that a N_S is strongly bound with a titanium

atom at the interstitial site (Ti$_i$), giving rise to a defect-impurity band thermally connected with the host VBM and eliminating the localized N$_S$-related states.[31] The suggested model mechanism gives a reasonable explanation for the photocatalytic oxidation reactions as well as the red-shift of the light absorption edge observed in N-doped TiO$_2$. In this La$_2$Ti$_2$O$_7$ system, we also investigated the electronic structure when N$_S$ and Ti$_i$ were bound together to form a complex defect. One Ti atom is inserted into the largest interstitial site in the 44-atom supercell so as to bring minimum lattice distortion to the system, as shown in Fig. 1(c). The point-defect formation energy was calculated using the formula:

$$E_{form} = E_D - E_H + \sum_i a_i n_i \mu_i \qquad (1)$$

where E_{form} is the point-defect formation energy, E_D is the total energy of the system containing point-defects, E_H is the total energy of the pristine system, $a_i = -1$ or 1 if an i atom is added or removed, n_i is the number of i atoms, and μ_i is the chemical potential of the i atom calculated using the method given in the ESI.†

The formation energy of N$_S$ + Ti$_i$ is plotted in Fig. S2 (ESI†). It can be seen that under O-poor and Ti-rich conditions, the formation energy is negative, which indicates that the N dopant and the interstitial Ti atoms are prone to co-exist. The formation energy comparison in Fig. S3 (ESI†) also indicates that formation of an interstitial Ti atom is energetically favourable when one oxygen atom is substituted by nitrogen atom under O-poor conditions.

When N$_S$ and Ti$_i$ co-existed, the electronic structures were very similar to the model where N solely doped with La$_2$Ti$_2$O$_7$, *i.e.*, localized mid-gap states formed as shown in Fig. 5 and Fig. S4 (ESI†). According to the hybrid results, the two localized energy bands, composed of mainly Ti 3d and the least O 2p states, covered a large range below the CBM, unlike the system with only the N$_S$ defect where one deep energy band lies in the middle of the band gap. Furthermore, the mixed N 2p and O 2p energy band (denoted L$_1$) was located at 0.4 eV above the VBM, rather than being close to the VBM as in the N mono-doped system. The hybridization among the N p and Ti d orbitals can be clearly observed using the partial electron densities in Fig. 5(c) and (d). The localized energy states were occupied, thus the Fermi level was substantially increased to just below the CBM. Again, the deep localized mid-gap energy states (denoted L$_2$) lead to low charge mobility and can act as the charge-carrier traps, which are unfavourable to the photocatalytic activity.[35] The DOS and the band structure obtained using the conventional DFT also indicated the formation of the localized energy state at 0.3 eV above the VBM (Fig. S4, ESI†).

Both DFT calculations and experiments have shown that nitrogen doping leads to formation of oxygen vacancies in bulk TiO$_2$.[36,37] The complex defects (N$_S$ + V_O) alter the band gap, and also cause the formation of a mid-gap localized energy state.[35,38,39] The 3d states of Ti^{3+} below the conduction band, which are associated with oxygen vacancies, have been found to act as the electron–hole recombination sites, leading to the
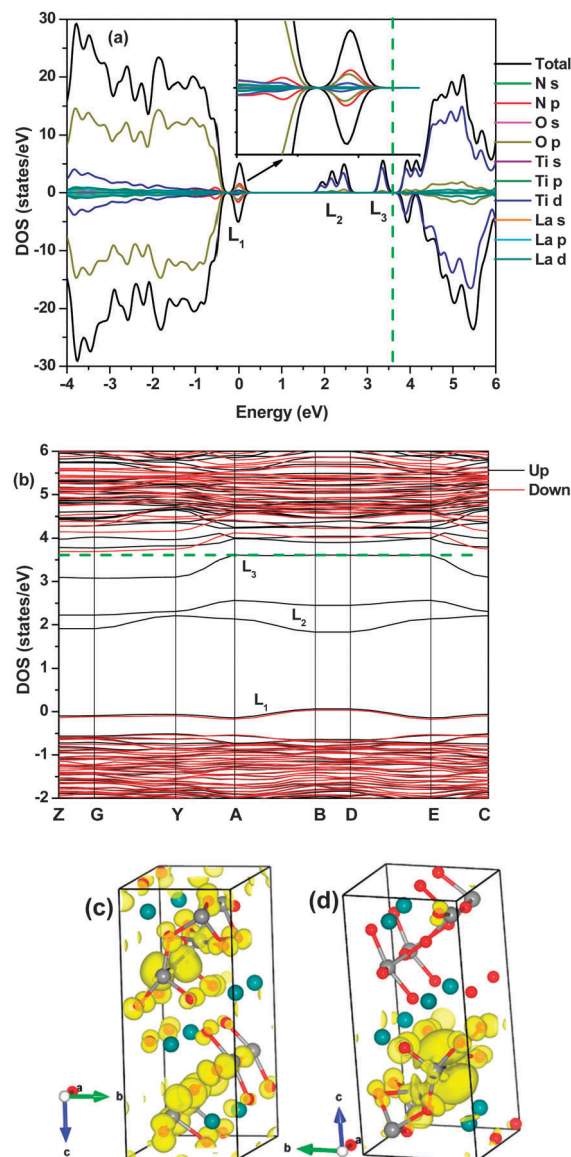

Fig. 5 DOS (a), band structure (b), partial electron densities of the VBM (c) and the localized energy level (L$_1$) at point *D* (d) at a 0.01 eV Å^{-3} isosurface level of La$_2$Ti$_2$O$_7$ with the N$_S$ and the Ti$_i$ defects in a supercell calculated using the HSE06 method. The dash line annotates the Fermi level.

reduction of photocatalytic activity.[35] Herein we also found that the formation energy was substantially reduced after V_O was introduced into the N-doped La$_2$Ti$_2$O$_7$ lattice (Fig. S3, ESI†), which indicated that oxygen vacancies were easily formed during the introduction of N into the lattice. But the influence of complex defects on the electronic structures was greatly different for La$_2$Ti$_2$O$_7$ and TiO$_2$. In order to achieve the charge neutrality, the model was built to contain two N$_S$ and one V_O (Fig. 1(d)). As shown in Fig. 6 and Fig. S5 (ESI†), the localized energy state completely disappeared when two N$_S$ co-existed with one V_O. The mixed N 2p, O 2p and Ti 3d orbitals formed a continual energy band on the top of the valence band (obtained using the HSE06 method) or thermally connected with the VBM (obtained using the conventional DFT), which accounted for
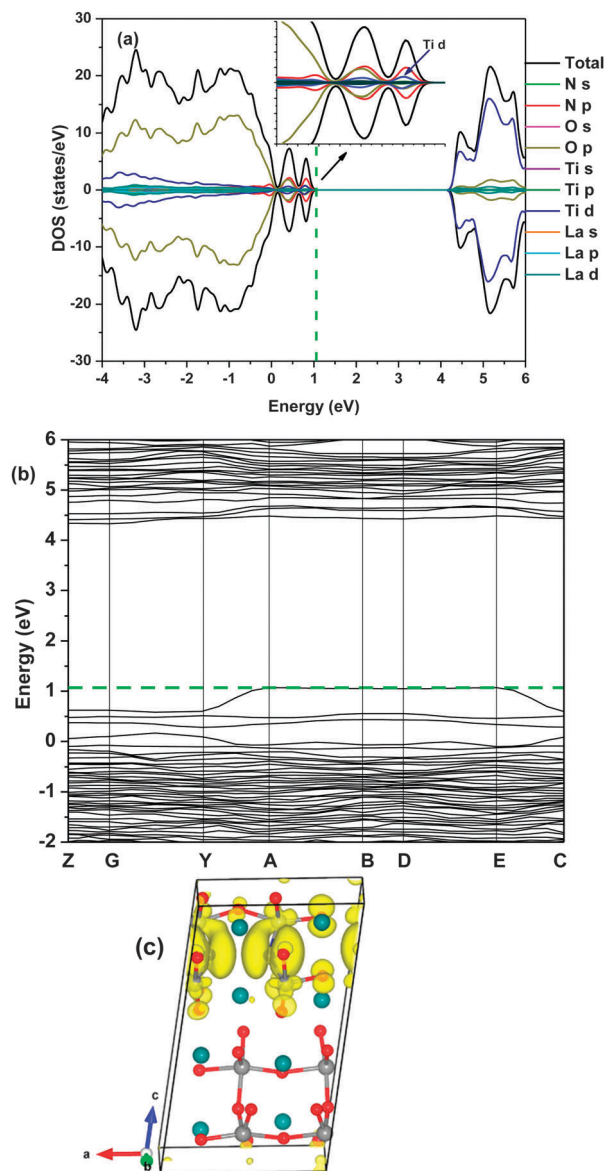
This journal is © the Owner Societies 2015

Phys. Chem. Chem. Phys., 2015, **17**, 8994–9000 | **8997**

Fig. 6 DOS (a), the band structure (b) and partial electron densities of the VBM at a 0.01 eV Å^{-3} isosurface level (c) of $La_2Ti_2O_7$ with two N_S and one V_O defects in a supercell calculated using the HSE06 method. The dash line annotates the Fermi level.
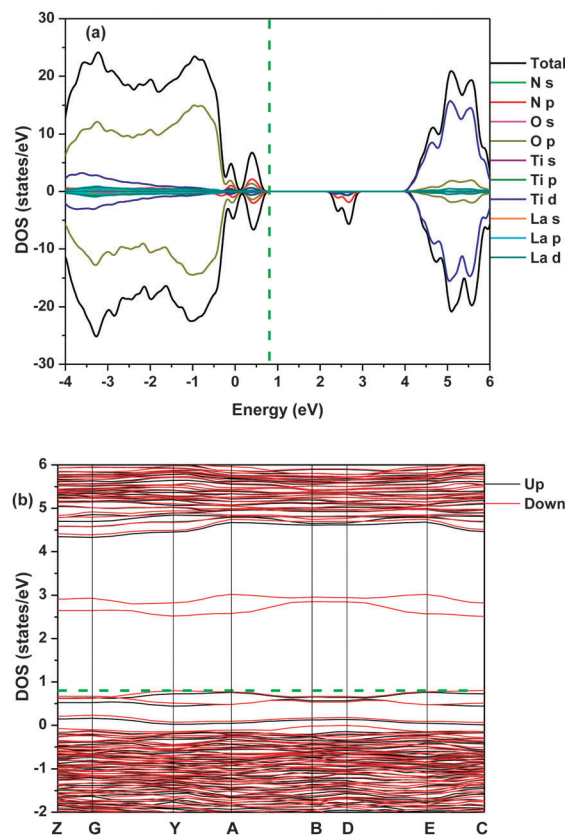

Fig. 7 DOS (a) and the band structure (b) of $La_2Ti_2O_7$ with two N_S defects in a supercell calculated using the HSE06 method. The dash line annotates the Fermi level.

the parallel red shift of the whole optical absorption edge of the N-doped sample.[13] The band gap was narrowed by 0.85 eV and 1.15 eV, which were determined by the conventional DFT and HSE06 approaches, respectively. For the HSE06 calculation result, the VBM shifted upwards by 1.07 eV while the CBM shifted downwards by 0.14 eV in comparison with pristine $La_2Ti_2O_7$. The VBM and CBM variation trends obtained using the theoretical calculation were in good agreement with the experimental results reported for the N-doped $La_2Ti_2O_7$ nanosheets.[13] As well, the added bands created a broad direct transition at a similar energy as the indirect band gap, improving the light absorption. This was in agreement with the added band edge as seen experimentally with N doping in $La_2Ti_2O_7$, wherein the absorption can be described by the superimposed direct and indirect band gaps.[13,21]

In TiO_2, the N dopant concentration has an effect on the electronic structure of N-doped TiO_2.[31] If a high concentration of N (e.g. 6.25 at%) was employed in the calculation, the N 2p state was mixed with O 2p, leading to band gap narrowing rather than localized deep energy state formation.[40] If a low concentration of N (e.g. 1.56 at%) was used in the calculation, a deep localized energy state formed in the forbidden band.[31,34,35] In order to study the influence of the nitrogen concentration on the electronic structure, we also investigated the DOS and the band structure of $La_2Ti_2O_7$ with 7.1 at% of N concentration, corresponding to the system containing two N_S and one V_O in a supercell in Fig. 1(d). By comparing Fig. 4 and 7, it can be confirmed that doping N alone into $La_2Ti_2O_7$ led to the formation of a localized deep energy state in the forbidden gap, independent of the concentration change. For the two systems containing either two N_S (Fig. 7 and Fig. S6, ESI†) or two N_S plus one V_O (Fig. 6 and Fig. S5, ESI†), the electronic structures were very similar, except that the localized deep energy state disappeared completely in the latter case. This has further confirmed that the localized energy state can be removed and the band gap be narrowed simultaneously only when N_S and V_O co-exist in $La_2Ti_2O_7$.

In comparison with the systems containing N_S and N_S + Ti_i, the Ti 4d orbitals contributed more to the VBM in $La_2Ti_2O_7$ containing both N_S and V_O, as clearly demonstrated by the DOS

8998 | Phys. Chem. Chem. Phys., 2015, 17, 8994–9000

This journal is © the Owner Societies 2015

shown in the inset of Fig. 6(a). This indicated that hybridization of orbitals between non-metals and metals was enhanced when N_S and V_O existed simultaneously, which can also be verified by the partial electron density of the VBM of $La_2Ti_2O_7$ containing different defects. In comparison with other configurations, strong orbital hybridization between N and Ti occurred in $La_2Ti_2O_7$ containing both N_S and V_O, as shown in Fig. 6(c). The extended nature of the valence band edge caused by the hybridized N 2p and Ti 3d states is beneficial to the migration of photo-induced holes, which increases the oxidation capability of the photocatalysts.[31,41] As a result, the N doped $La_2Ti_2O_7$ nanosheets perform well in photocatalytic decomposition of methyl orange.[13] N doping is an effective method to realize the visible light photocatalytic activity. In short, if N doping into $La_2Ti_2O_7$ occurs in a reducing atmosphere, the presence of V_O will reduce the band gap and eliminate the localized energy state, leading to enhancement in the photocatalytic activity in both the ultraviolet and visible light regions.

4. Conclusions

The conventional DFT and HSE06 hybrid methods were employed to investigate the influence of the N substitutions co-existing with the oxygen vacancy and the interstitial Ti atom on the electronic structures. Doping N alone into $La_2Ti_2O_7$ caused the formation of the deep localized energy state, independent of the doping concentration. When interstitial Ti co-existed with N_S, the localized energy state was still present. However, when N_S co-existed with V_O, the localized energy state was completely removed and the band gap can be substantially narrowed. Furthermore, the added DOS altered the VBM, which facilitated the migration of photo-induced holes and the oxidation power of the photocatalyst, introduced optical transitions at lower energy to increase light absorption. As a result, the N_S plus V_O model in $La_2Ti_2O_7$ can accurately interpret the fact that N doping into $La_2Ti_2O_7$ can not only lead to strong visible light photocatalytic activity but also enhance the performance under UV irradiation. This work reveals that tuning the non-neutral point defects with the oxygen vacancy is an effective strategy for alleviating the problem associated with doping to increase light absorption, which have implications in engineering the band gap of semiconductor photocatalysts.

Acknowledgements

Notes and references

1 K. Honda and A. Fujishima, *Nature*, 1972, **238**, 37.
2 H. Tong, S. X. Ouyang, Y. P. Bi, N. Umezawa, M. Oshikiri and J. H. Ye, *Adv. Mater.*, 2012, **24**, 229.
3 J. Y. Li and N. Q. Wu, *Catal. Sci. Technol.*, 2015, **5**, 1360.
4 A. Kudo and Y. Miseki, *Chem. Soc. Rev.*, 2009, **38**, 253.
5 H. G. Kim, D. W. Hwang, J. Kim, Y. G. Kim and J. S. Lee, *Chem. Commun.*, 1999, 1077.
6 X. C. Wang, K. Maeda, A. Thomas, K. Takanabe, G. Xin, J. M. Carlsson, K. Domen and M. Antonietti, *Nat. Mater.*, 2009, **8**, 76.
7 Y. Miseki, H. Kato and A. Kudo, *Energy Environ. Sci.*, 2009, **2**, 306.
8 R. Abe, M. Higashi, K. Sayama, Y. Abe and H. Sugihara, *J. Phys. Chem. B*, 2006, **110**, 2219.
9 T. Takata, Y. Furumi, K. Shinohara, A. Tanaka, M. Hara, J. N. Kondo and K. Domen, *Chem. Mater.*, 1997, **9**, 1063.
10 Y. F. Huang, Y. L. Wei, S. H. Cheng, L. Q. Fan, Y. B. Li, J. M. Lin and J. H. Wu, *Sol. Energy Mater. Sol. Cells*, 2010, **94**, 761.
11 K. W. Li, Y. Wang, H. Wang, M. K. Zhu and H. Yan, *Nanotechnology*, 2006, **17**, 4863.
12 Q. L. Yang, S. Z. Kang, H. Chen, W. B. Bu and J. Mu, *Desalination*, 2011, **266**, 149.
13 F. K. Meng, Z. L. Hong, J. Arndt, M. Li, M. J. Zhi, F. Yang and N. Q. Wu, *Nano Res.*, 2012, **5**, 213.
14 Q. Wang, T. Hisatomi, Y. Moriya, K. Maeda and K. Domen, *Catal. Sci. Technol.*, 2013, **3**, 2098.
15 D. W. Hwang, H. G. Kim, J. S. Jang, S. W. Bae, S. M. Ji and J. S. Lee, *Catal. Today*, 2004, **93–95**, 845.
16 D. Arney, B. Porter, B. Greve and P. A. Maggard, *J. Photochem. Photobiol., A*, 2008, **199**, 230.
17 D. W. Hwang, H. G. Kim, J. S. Lee, J. Kim, W. Li and S. H. Oh, *J. Phys. Chem. B*, 2005, **109**, 2093.
18 Z. M. Shao, S. Saitzek, P. Roussel, A. Ferri, Ol. Mentré and R. Desfeux, *CrystEngComm*, 2014, **16**, 8517.
19 A. Nashim, S. Martha and K. M. Parida, *RSC Adv.*, 2014, **4**, 14633.
20 S. J. Hu, L. C. Jia, B. Chi, J. Pu and L. Jian, *J. Power Sources*, 2014, **266**, 304.
21 F. K. Meng, J. T. Li, Z. L. Hong, M. J. Zhi, A. Sakla, C. C. Xiang and N. Q. Wu, *Catal. Today*, 2013, **199**, 48.
22 P. Liu, J. Nisar, B. Pathak and R. Ahuja, *Phys. Chem. Chem. Phys.*, 2013, **15**, 17150.
23 P. Liu, J. Nisar, B. S. Sa, B. Pathak and R. Ahuja, *J. Phys. Chem. C*, 2013, **117**, 13845.
24 G. Kresse and J. Furthmüller, *Phys. Rev. B: Condens. Matter Mater. Phys.*, 1996, **54**, 11169.
25 J. P. Perdew, K. Burke and M. Ernzerhof, *Phys. Rev. Lett.*, 1996, **77**, 3865.
26 J. Heyd, G. E. Scuseria and M. Ernzerhof, *J. Chem. Phys.*, 2003, **118**, 8207.
27 G. Kresse and D. Joubert, *Phys. Rev. B: Condens. Matter Mater. Phys.*, 1999, **59**, 1758.
28 H. W. Schmalle, T. Williams and A. Reller, *Acta Crystallogr., Sect. B: Struct. Sci.*, 1993, **49**, 235.

This journal is © the Owner Societies 2015

Phys. Chem. Chem. Phys., 2015, **17**, 8994–9000 | 8999

29 L.J. Sham and M. Schlüter, *Phys. Rev. Lett.*, 1983, **51**, 1888.

30 L. J. Sham and M. Schlut, *Phys. Rev. B: Condens. Matter Mater. Phys.*, 1985, **32**, 3883.

31 N. Umezawa and J. H. Ye, *Phys. Chem. Chem. Phys.*, 2012, **14**, 5924.

32 C. D. Valentin, G. Pacchioni and A. Selloni, *Phys. Rev. B: Condens. Matter Mater. Phys.*, 2004, **70**, 085116.

33 Z. Lin, A. Orlov, R. M. Lambert and M. C. Payne, *J. Phys. Chem. B*, 2005, **109**, 20948.

34 J. B. Varley, A. Janotti and C. G. Van de Walle, *Adv. Mater.*, 2011, **23**, 2343.

35 J. Wang, D. N. Tafen, J. P. Lewis, Z. L. Hong, A. Manivannan, M. J. Zhi, M. Li and N. Q. Wu, *J. Am. Chem. Soc.*, 2009, **131**, 12290.

36 C. D. Valentin, G. Pacchioni, A. Selloni, S. Livraghi and E. Giamello, *J. Phys. Chem. B*, 2005, **109**, 11414.

37 M. Batzill, E. H. Morales and U. Diebold, *Phys. Rev. Lett.*, 2006, **96**, 026103.

38 H. C. Wu, Y. S. Lin and S. W. Lin, *Int. J. Photoenergy*, 2013, **2013**, 289328.

39 P. P. González-Borrero, H. S. Bernabé, N. G. C. Astrath, A. C. Bento, M. L. Baesso, M. V. Castro Meira, J. S. de Almeida and A. Ferreira da Silva, *Appl. Phys. Lett.*, 2011, **99**, 221909.

40 K. Aoki and Y. Taga, *Science*, 2001, **293**, 269.

41 H. Kawazoe, H. Yanagi, K. Ueda and H. Hosono, *MRS Bull.*, 2000, **25**, 28.

9000 | *Phys. Chem. Chem. Phys.*, 2015, **17**, 8994–9000

This journal is © the Owner Societies 2015